Melt Rheology and Morphology of LLDPE/EVA Blends: Effect of Blend Ratio, Compatibilization, and Dynamic Crosslinking

K. A. Moly,[1] Z. Oommen,[2] S. S. Bhagawan,[3] G. Groeninckx,[4] S. Thomas[5]

[1]*B K. College, Amalagiry P.O., Kottayam, Kerala, India*
[2]*CMS College, Kottayam, Kerala, India*
[3]*Propellent Engineering Division, Vikram Sarabhai Space Centre Thiruvananthapuram 695022*
[4]*Katholieke Univ Leuven, Department of Chemistry, Lab Macromol Struct Chem, Celestijnenlaan 200F, B-3001 Heverlee, Belgium*
[5]*School of Chemical Sciences, Mahatma Gandhi University, Priyadharshini Hills, P.O. Kottayam 686560 Kerala, India*

ABSTRACT: The melt rheological properties of linear low-density polyethylene (LLDPE)/ethylene vinyl acetate (EVA) blends were investigated with special reference to the effect of blend ratio, temperature, shear rate, compatibilization, and dynamic vulcanization. The melt viscosity of the blends determined with a capillary rheometer is found to decrease with an increase of shear rate, which is an indication of pseudoplastic behavior. The viscosity of the blend was found to be a nonadditive function of the viscosities of the component polymers. A negative deviation was observed because of the interlayer slip between the polar EVA and the nonpolar LLDPE phases. The melt viscosity of these blends decreases with the increased concentration of EVA. The morphology of the extrudate of the blends at different shear rates and blend ratios was studied and the size and distribution of the domains were examined by scanning electron microscopy. The morphology was found to depend on shear rate and blend ratio. Compatibilization of the blends with phenolic- and maleic-modified LLDPE increased the melt viscosity at lower wt % of compatibilizer and then leveled off. Dynamic vulcanization is found to increase the melt viscosity at a lower concentration of DCP. The effect of temperature on melt viscosity of the blends was also studied. Finally, attempts were made to correlate the experimental data on melt viscosity and cocontinuity region with different theoretical models. © 2002 Wiley Periodicals, Inc. J Appl Polym Sci 86: 3210–3225, 2002

Key words: rheology; compatibilization; crosslinking; modeling; blends; morphology

INTRODUCTION

Knowledge of the flow behavior of polymer blends is of great importance to optimize processing conditions. The flow behavior of homopolymers depends on the molecular characteristics, flow geometry, and processing conditions such as temperature, shear rate, time of flow, etc. In polymer blends, the flow behavior is controlled by certain additional factors such as interfacial adhesion, interfacial thickness, miscibility, and morphology of the system. Several research works were carried out to analyze the complicated rheological behavior of polymers because of its importance in processing.[1–4] Basic information about the influence of the different parameters on viscosity, processing, elasticity, and extrudate characteristics will be a guideline in the selection of proper polymer under a given set of processing conditions.[5] In recent years, the melt flow behavior of thermoplastic elastomers from rubber/plastic blends has received a lot of attention. Danesi and Porter[6] studied the rheological behavior of polypropylene and ethylene propylene rubber. Various researchers[7] analyzed the rheological behavior of many polymer blends. Kim and coworkers[8] studied the properties of miscible and immiscible blends of poly(methyl methacrylate) (PMMA)/acrylonitrile-butadiene-styrene copolymer (ABS) with ABS having different acrylonitrile content. The rheological analysis of these blends revealed that the viscosities of the miscible blends are lower than the additive values because of dilution effects, where as immiscible blends with ABS rich phase showed positive deviation.

In this laboratory, Thomas and coworkers[9–12] studied the flow behavior of various thermoplastic elastomers. Increase in viscosity upon the incorporation of rubber in a plastic phase was reported in systems such as plasticized poly(vinyl chloride) (PVC)/epoxidized natural rubber (ENR), polypropylene (PP)/NR, high-density polyethylene (HDPE)/NR, and PP/ethylene–propylene–diene rubber (EPDM).[13–18]

Compatibilizers are used to improve the properties of immiscible polymer blends. The addition of compatibilizers to polymer blends affects the flow behavior because of the interactions occurring between the components of blend upon compatibilization.[19–23] Recently, in this laboratory the flow behavior of PMMA/NR blends compatibilized with poly(methyl methacrylate)-grafted natural rubber (PMMA-g-NR) copolymer was investigated.[23] At low shear rates, the binary blends showed positive deviation. Upon compatibilization, the blends showed positive deviation because of high interfacial interaction. Various researchers analyzed the viscosity of immiscible polymer blends by using different rheological models for the flow behavior.[24] These models reveal that the blend has contributions from the viscosities of the pure components and also from the viscosity of the interface.

The effect of dynamic vulcanization on the rheological behavior of rubber–plastic blends was studied by several researchers.[25–28] It was reported that the viscosity of the blends increased with increasing curative concentration.[25] Kuriakose et al. studied the effect of various vulcanizing agents on the rheological behavior of PP/NR and HDPE/NR blends.[15,26]

Linear low-density polyethylene/ethylene vinyl acetate (LLDPE/EVA) blends have many industrial uses because of their good mechanical strength, processibility, impact strength, insulation properties, etc. To our knowledge, so far no attempts have been made to study the rheological properties of these blends. In this article, we have investigated the rheological properties of LLDPE/EVA blends. The effects of blend ratio, compatibilization, and dynamic vulcanization on the flow characteristics have been studied. The extrudate morphology was examined and correlated with the flow properties.

EXPERIMENTAL

Materials

LLDPE (Reclair F19010) with a density of 0.92 g/mL and a melt flow index of 0.90 g/10 min was procured from Reliance Industries Ltd., Hazira, Gujarath, India. EVA (Piolene 1802) of vinyl acetate content of 18%, density of 0.93 g/mL, and melt flow index of 2 g/10 min was procured from PIL, Madras, India. The compatibilizer MA-g-LLDPE was prepared by melt mixing LLDPE (100 parts) with maleic anhydride (5 parts) and benzoyl peroxide (0.5 g) at 125°C. Phenolic-modified compatibilizer was also prepared by melt mixing. LLDPE (100 parts) was mixed with phenolic resin (4 parts) and stannous chloride (0.8 g) at 125°C.

Preparation of the blends

The blends of LLDPE/EVA were prepared in a Brabender plasticorder at 125°C by using a rotor speed of 60 rpm. LLDPE was melted first for 2 min, and then EVA was added and mixed for 4 min. The total mixing time was 6 min in all cases. The blends having different compositions were designated E_x (x = 0, 30, 50, 70, 100), where x represents the weight percentage of EVA in the blend. The compatibilized 70/30 LLDPE/EVA blends with 0, 0.5, 2.5, and 10 wt % of maleic-modified compatibilizer are represented as 3E, 0.5 MC, 2 MC, 5 MC, and 10 MC, respectively. The 70/30 LLDPE/EVA blends with phenolic-modified compatibilizer are depicted as 0.5 PC, 2 PC, 5 PC, and 10 PC. The dynamically vulcanized 70/30 EVA/LLDPE blends were prepared by melt mixing EVA (70 parts) and LLDPE (30 parts) with DCP wt % (based on the weight of EVA) 0, 1, 2, 3, and 4 and they are designated 7E, 7EC1, 7EC2, 7EC3, and 7EC4, respectively.

Rheological measurements

The shear viscosities of the blends were measured in a Gottfert 2002 capillary rheometer. A capillary having a l/d ratio of 30 and an angle of entry of 180° was used. The experiments were done at three different temperatures of 140, 150, and 160°C with different shear rates ranging from 5 to 300 s^{-1}. Apparent shear rate (γ_{app}) and shear stress (τ_{app}) were recorded from the recorder assembly.

From the apparent shear rate values, the true shear rate (γ_w) was calculated by using the following equation, which includes the Rabinowitch correction[5]:

$$\dot{\gamma}_w = \frac{(3n' + 1)}{4n'} \dot{\gamma}_{app} \tag{1}$$

where n' is the flow behavior index. n' is defined as

$$n' = \frac{d(\log \tau_w)}{d(\log \dot{\gamma}_{app})} \tag{2}$$

The flow behavior index (n') was obtained by regression analysis based on the values of the τ_w and γ_{app} obtained from the experimental data. The shear viscosity η was calculated as

$$\eta = \frac{\tau_w}{\dot{\gamma}_w} \tag{3}$$

Extrudate morphology

The morphology of the extrudate was studied by SEM analysis. For this, the cryogenically fractured surface

of the extrudate was sputter coated with gold and examined under a scanning electron microscope.

The extrudate morphology of polymer blends is influenced by composition, viscosity of component polymers, interfacial tension, and shear rate. When the polymers have similar melt viscosities, the minor component is finely and uniformly distributed in the major component.[6] When the two polymers have different melt viscosities, the morphology of the blend depends on whether the minor component has lower or higher melt viscosity than the major component. Normally, the least viscous component forms the continuous phase irrespective of composition.[29] In LLDPE/EVA blends, EVA and LLDPE exhibit similar viscosities.

General observations of the morphology of the blends reveal a decrease in particle size with an increase in shear rate. The decrease in particle size with an increase in shear rate is due to the deformation and breakdown of particles in the capillary by the action of shear force. The size of the dispersed domain measured from SEM may be expressed in different ways, such as,

$$\bar{D}_n = \frac{\sum N_i D_i}{\sum N_i} \qquad (4)$$

$$\bar{D}_w = \frac{\sum N_i D_i^2}{\sum N_i D_i} \qquad (5)$$

$$\bar{D}_{vs} = \frac{\sum N_i D_i^4}{\sum N_i D_i^3} \qquad (6)$$

where N_i is the number of domains having diameter D_i, D_n is the number-average diameter, D_w is the weight average diameter, and D_{vs} is the surface-area average diameter. The polydispersity index, which is a measure of domain distribution, was also calculated from

$$\mathrm{PDI} = \dot{\bar{D}}_w / \bar{D}_n \qquad (7)$$

More than 500 domains were considered from different micrographs for calculating the domain diameter. The interfacial area per unit volume of the blends was calculated by using the relation
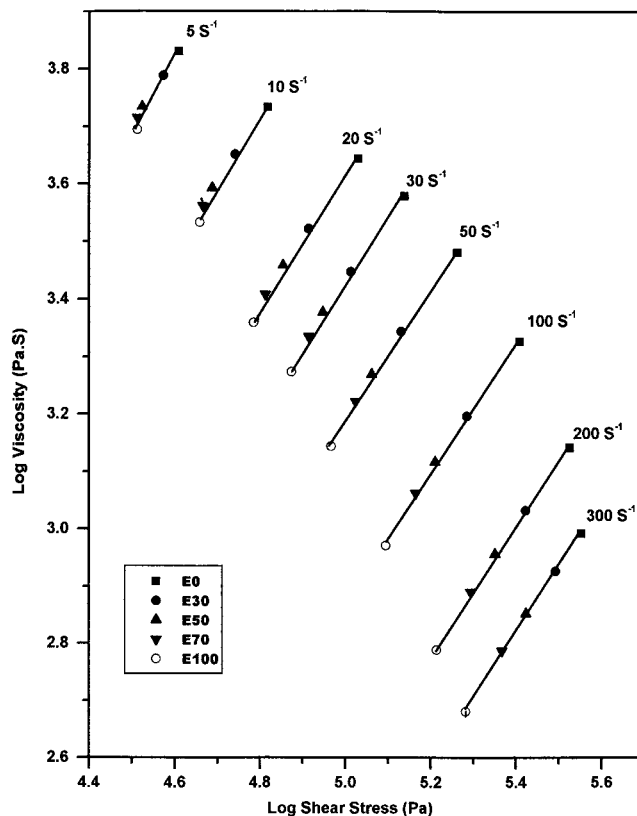
$$\mathrm{Interfacial\ area/unit\ volume} = 3\phi_A/R \qquad (8)$$

where ϕ_a represents the volume fraction of the dispersed phase and R is the dispersed domain diameter.

RESULTS AND DISCUSSION

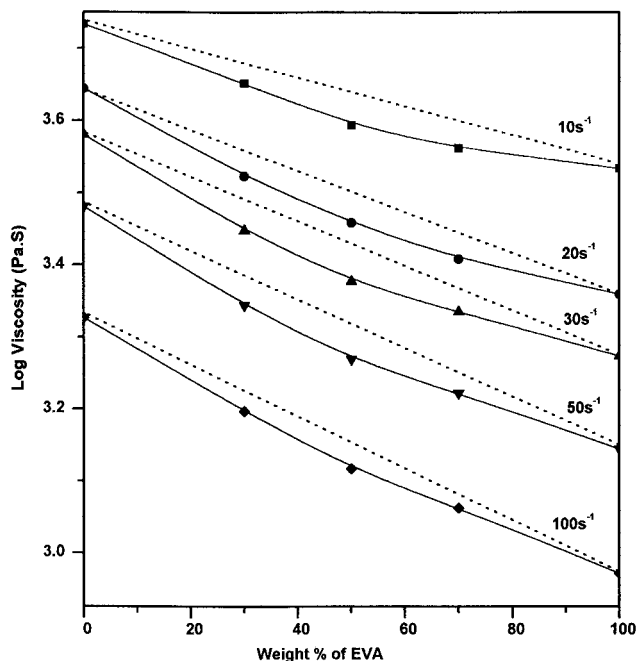### Effects of blend ratio on melt viscosity

The dependence of viscosity of LLDPE/EVA blends on shear stress at different shear rates at 150°C is

Figure 1 Effect of shear stress on viscosity of LLDPE/EVA blends at different shear rates and at 150°C.

represented in Figure 1. The viscosity of all the blends decreases with shear stress, which is an indication of pseudoplastic behavior. Under the application of shear stress, the entangled polymer chains undergo disentanglement and orientation, resulting in a decrease of viscosity and pseudoplastic behavior. At practically zero shear stress, the molecules are randomly oriented and entangled, which results in high viscosity. At a given shear stress, the viscosity values decrease with an increase in concentration of EVA. At low shear rates, E_{100} and E_{70} show nearly equal viscosities. At high shear rates, the viscosities are quite different.

The dependence of viscosity of LLDPE/EVA blends on EVA content at different shear rates is shown in Figure 2. It is observed that the viscosity decreases with an increase in EVA content. Further, the viscosity values of the blends show negative deviation from the additivity line, which indicates the incompatibility of the system. When a shear force is applied to the blend, it undergoes an elongational flow. If the interface is strong, deformation of the dispersed phase would be effectively transferred to the continuous phase. However, in the case of weak interfaces, interlayer slip occurs and this is responsible for the negative deviation of the viscosity from the additivity line.[30] Such a

**Figure 2** Effect of blend ratio on viscosity of LLDPE/EVA blends at 150°C.

behavior may also be explained on the basis of the morphology of the LLDPE/EVA system. It can be seen that there is a decrease in viscosity up to E_{50}. After that, the decrease in viscosity is not so sharp. Such a behavior can be correlated with the morphology of the

system. SEM micrographs of cross sections of the extrudates of LLDPE/EVA blends are given in Figure 3. The blend E_{30} shows a two-phase morphology where EVA is the dispersed phase and LLDPE forms the matrix, whereas E_{50} shows a cocontinuous morphology. E_{70} also has a two-phase morphology where EVA forms the continuous matrix and LLDPE forms the dispersed phase. Viscosity of all the blends shows a negative deviation from additivity line and may be due to the poor interaction between the two phases and the consequent interlayer slip. Many researchers have reported such negative deviations.[31–33] Utracki and Sammut[34] showed that positive or negative deviation of measured viscosity from that calculated from the log additivity rule is an indication of strong or weak interaction between the phases of the blend. According to them,

$$In(\eta_{app})_{blend} = \sum_i W_i ln(\eta_{app})_i \qquad (9)$$

where W_i is the weight fraction of the ith component of the blend. They indicated that immiscible blends show negative deviation because of the heterogeneous nature of the components, whereas positive deviation is expected for blends because of the high stability and homogeneous nature of the components.

The following different theoretical models were used to calculate the viscosity of the blends at shear rate of 100 S^{-1}:

E_{30}

E_{50}

E_{70}
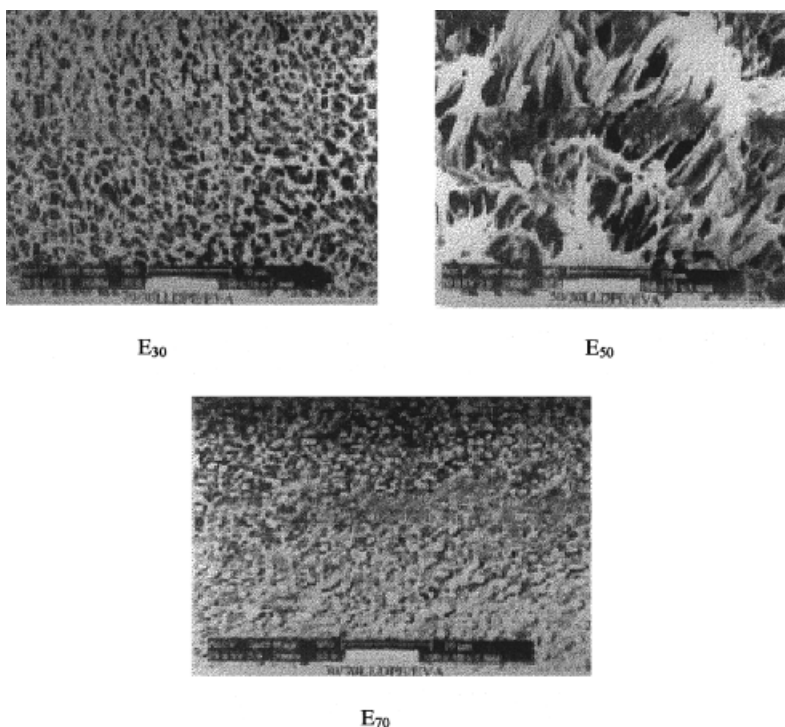
Figure 3 Effect of blend composition on the extrudate morphology of LLDPE/EVA blends at 150°C.

$$\eta = \eta_1\phi_1 + \eta_2\phi_2 \quad \text{(Model I)} \tag{10}$$

where ϕ_1 and ϕ_2 are the volume fractions of the components and η_1 and η_2 are the viscosities. Viscosity can also be calculated by using Hashin's upper and lower limit models[35]:

$$\eta_{\text{mix}} = \eta_2 + \frac{\phi_1}{1/(\eta_1 - \eta_2) + \phi_2/2\eta_2} \quad \text{(Model II)} \tag{11}$$

$$\eta_{\text{mix}} = \eta_1 + \frac{\phi_2}{1/(\eta_2 - \eta_1) + \phi_1/2\eta_1} \quad \text{(Model III)} \tag{12}$$

where $\eta_1, \eta_2, \phi_1,$ and ϕ_2 have the same meaning as before.

An altered free-volume model developed by Sood et al.[36] was also used to calculate the viscosity. According to the equation

$$\ln \eta_{\text{mix}} = \frac{\phi_1(\alpha - 1 - \gamma\phi_2)\ln \eta_1 + \alpha\phi_2(\alpha - 1 + \gamma\phi_1)\ln \eta_2}{\phi(\alpha - 1 - \gamma\phi_2) + \alpha\phi_2(\alpha - 1 + \gamma\phi_1)}$$

$$\text{(Model IV)} \tag{13}$$

where

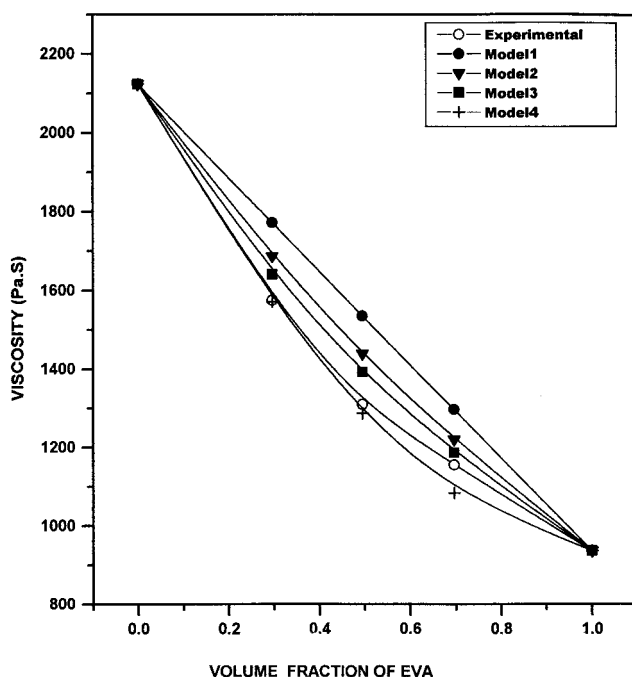$$\alpha = f_2/f_1 \tag{14}$$

and

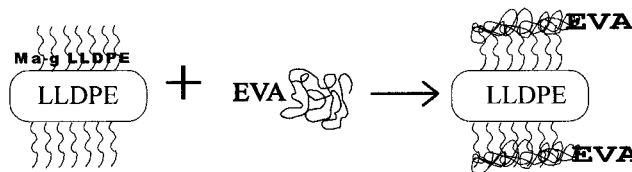**Figure 4** Theoretical and experimental viscosities of LLDPE/EVA blends.

Figure 5 Schematic representation of brush theory of compatibilization.

$$\gamma = \beta/f_1 \tag{15}$$

f_1 and f_2 are free volume fractions of components 1 and 2, respectively, and β is an interaction parameter

$$f = fg + \alpha_f(T - T_g) \tag{16}$$

where $f_g = 0.025$

$$f_g = 0.025$$

$$\alpha_f = B/2.303C_1C_2 \tag{17}$$

where $B = 0.9 \pm 0.3 \approx 1$, $C_1 = 17.44$, and $C_2 = 51.6$ K.

For the calculations, the value of γ was varied to obtain best fit values with that of experimental results. The viscosity data of LLDPE/EVA blends based on the various theoretical models are compared with experimental results in Figure 4. It is observed that the melt viscosity data calculated by using the Sood model lie closer to the experimental values. The viscosity values can be well explained by using the Sood model with $\gamma = -0.30$. This value of γ corresponds to an interaction parameter $\beta = -4.731 \times 10^{-2}$ according to eq. (15).

Effect of compatibilization

The physical and mechanical properties of immiscible blends are found to improve by the addition of block copolymers, graft copolymers, or modified polymers.[37,38] A suitably selected compatibilizer will locate at the interface by reducing the interfacial tension and increasing the interfacial adhesion. According to the brush theory, the interdiffusion between neighboring polymers resulting in entanglement of polymer chains is of great importance for bonding between phases.[39,40] The presence of compatibilizers increases interfacial thickness and this effect is related to the molecular weight of the surface-attached compatibilizer.[41] The thickest interface was observed for the compatibilizer having highest molecular weight. When the length of fully stretched compatibilizer chains are compared to the thickness of the interfaces, the interfaces are found to be thicker than the length of the compatibilizer chains.[42] This observation points to the
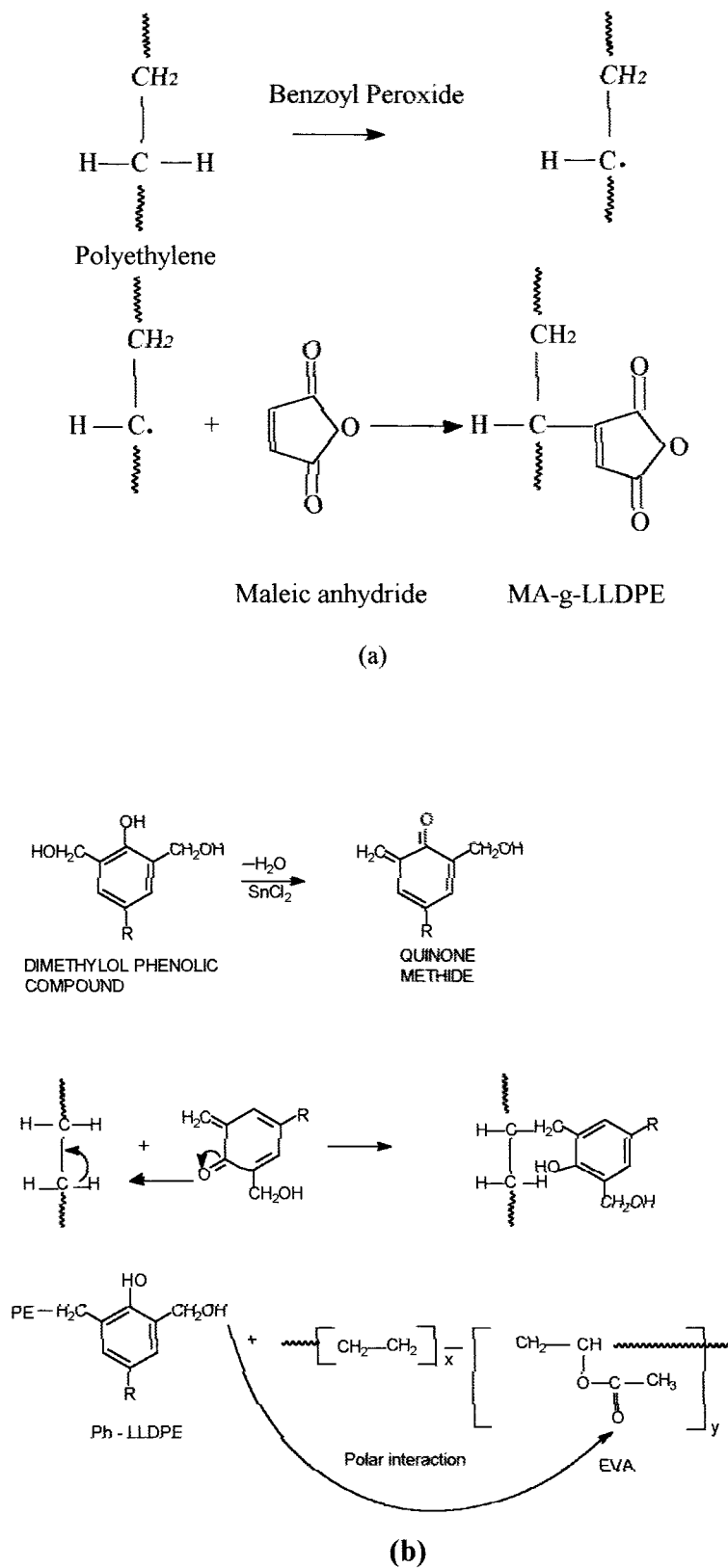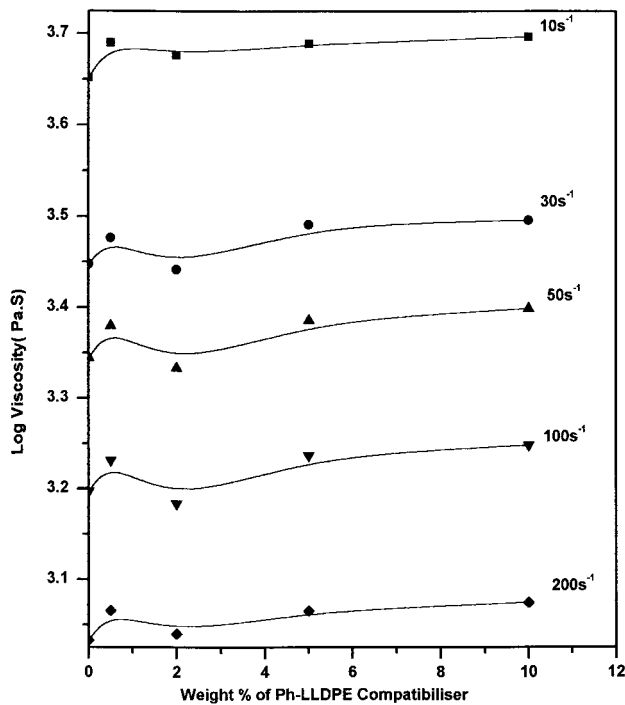
Figure 6 (a) Probable modification of LLDPE in the presence of maleic anhydride. (b) Probable mechanism of compatibilization of LLDPE/EVA blends in the presence of Ph-*g*-LLDPE.
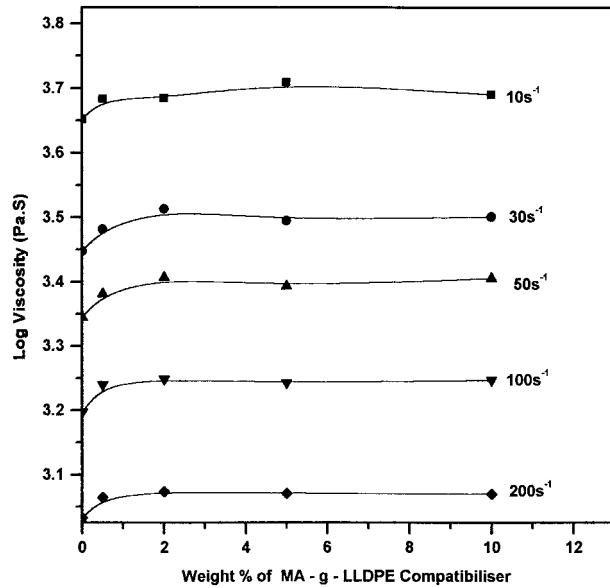
Figure 7 Variation of viscosity of E_{30} blend with MA-g-LLDPE compatibilizer concentration at different shear rates and at 150°C.

fact that the compatibilizer chains restrict the mobility of the matrix chains with which they are not in direct contact. There may be a probable stretching of the compatibilizer chains away from the matrix, forming a brushlike structure, which can be schematically repre-

sented as shown in Figure 5. The hydrophobic LLDPE chains of compatibilizer prefer to interact with LLDPE matrix and to be repelled by polar EVA phase. The polar maleic anhydride part of the compatibilizer interacts with the EVA phase.

The role of phenolic-modified LLDPE and maleic-modified LLDPE as compatibilizers in LLDPE/EVA blends is also investigated and compared. The probable mechanism of modification of LLDPE by grafting maleic unhydride is given in Figure 6(a) and the expected mechanism of compatibilization of LLDPE/EVA blends by using Ph-LLDPE is given in Figure 6(b), respectively. Upon the addition of Ph-LLDPE, the interfacial thickness increases, which leads to effective stress transfer between the dispersed phase and the continuous phase and an increase in interfacial adhesion. This contributes to the reduction in interlayer slip, thereby increasing the viscosity.

The variation of viscosity as a function of compatibilizer loading is given in Figures 7 and 8. The viscosity increases initially with an increase in compatibilizer loading and then levels off. Increases in viscosity of immiscible polymer blends upon compatibilization was reported by many researchers.[19–23] The viscosity of polymer blend has contribution from interface. For uncompatibilized blends, the final particle size increases with the dispersed phase concentration be-

Figure 8 Variation of viscosity of E_{30} blend with Ph-LLDPE compatibilizer concentration at different shear rates and at 150°C.
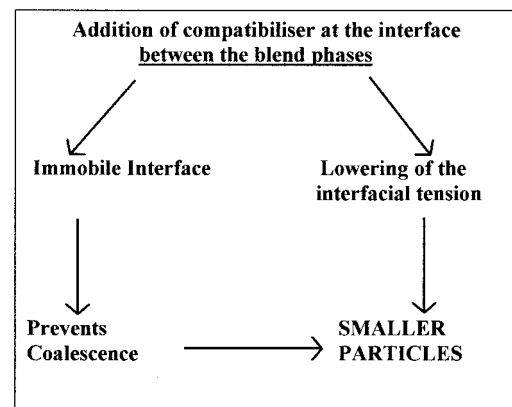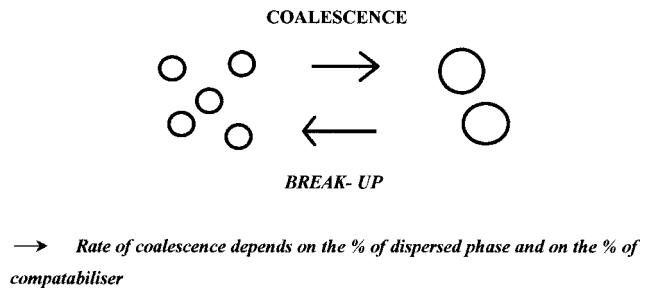
Figure 9 Schematic representation of the effect of interfacial compatibilization on phase morphology blends.
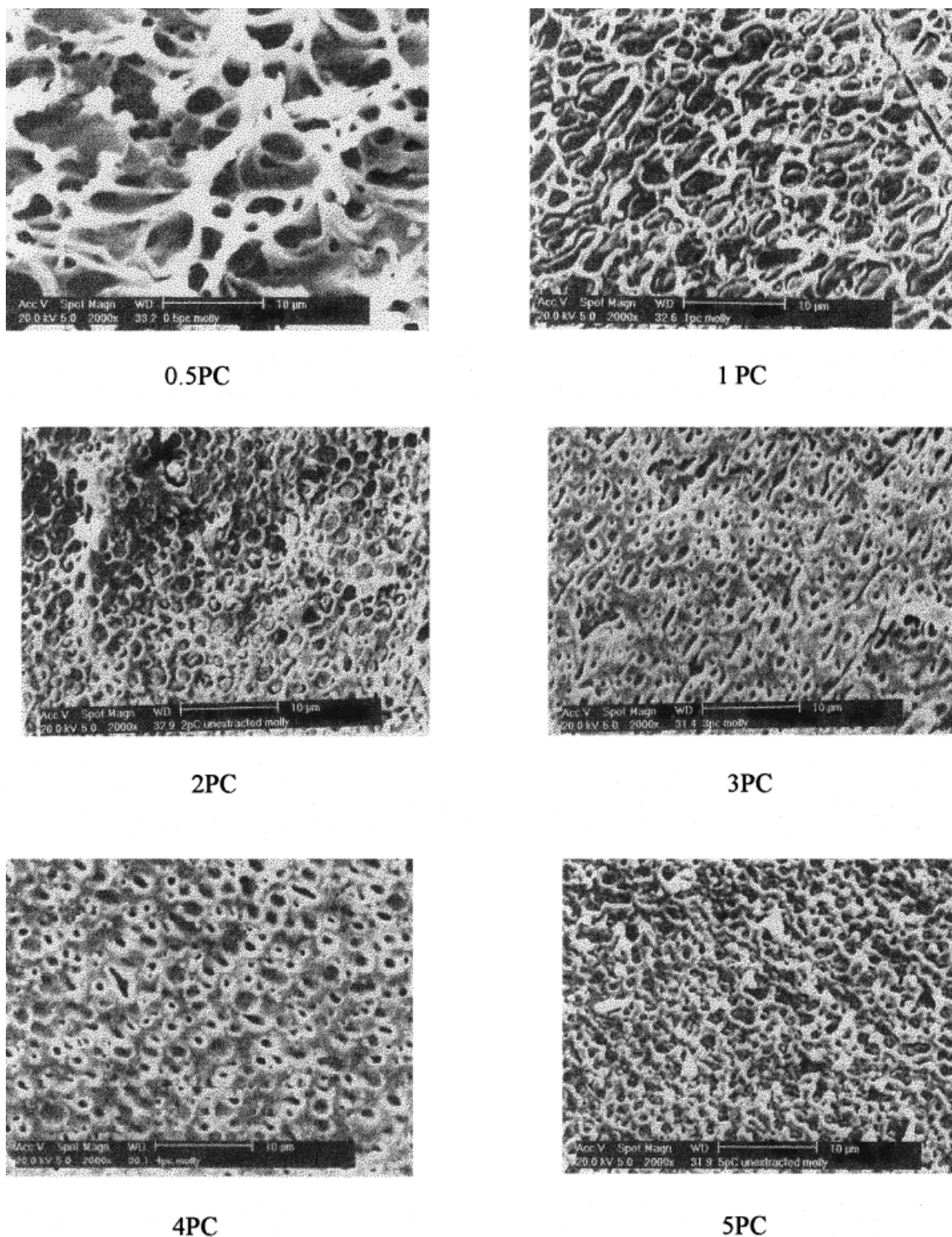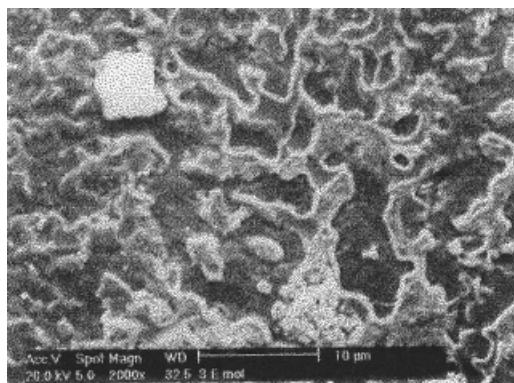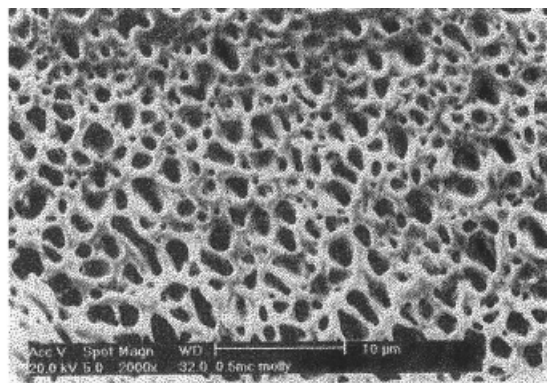
Figure 10 SEM of 70/30 LLDPE/EVA blends compatibilized with MA-*g*-LLDPE.

cause of increased coalescence. The particle size distribution also broadens at higher concentrations. It is shown that the main advantages of using compatibilizers in polymer blends is the suppression of coales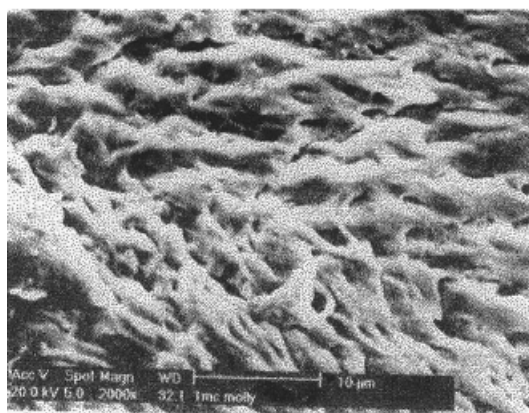cence achieved through stabilizing the interface, and also a reduction in the interfacial tension.[43] A schematic representation of the effect of interfacial compatibilization on phase morphology is given in Figure 9. The addition of compatibilizing agents results in a large reduction of the dispersed phase particle size.
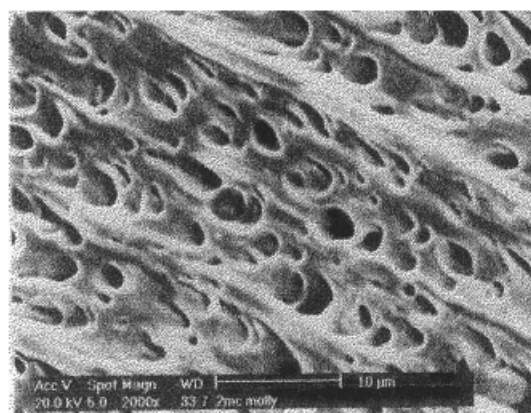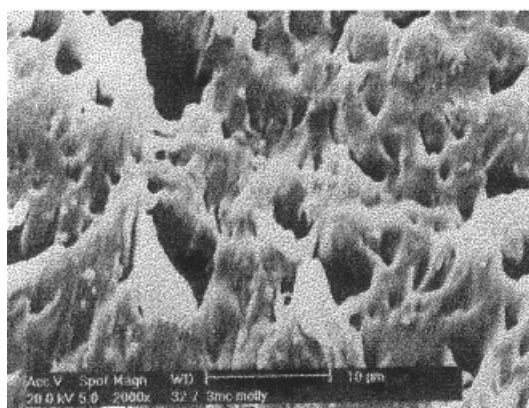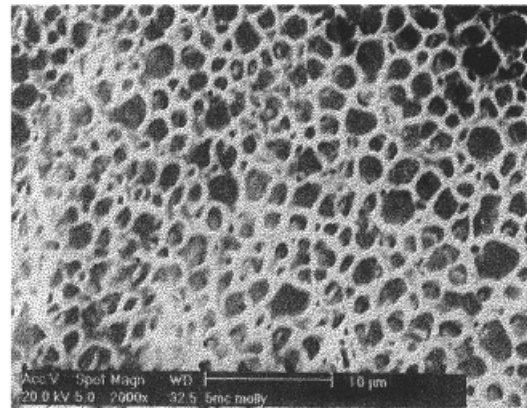
Figure 11 SEM of 70/30 LLDPE/EVA blends compatibilized with Ph-LLDPE.

The properties of the blends level off after a compatibilizer concentration of 3 wt %.[44] Upon compatibilization, the compatibilizer will locate at the interface between matrix and the dispersed phase by increasing the interfacial thickness and adhesion, thereby interlayer slip is decreased and viscosity is increased. According to Okoroafar et al.,[24] the viscosity of the compatibilized blend is given by:
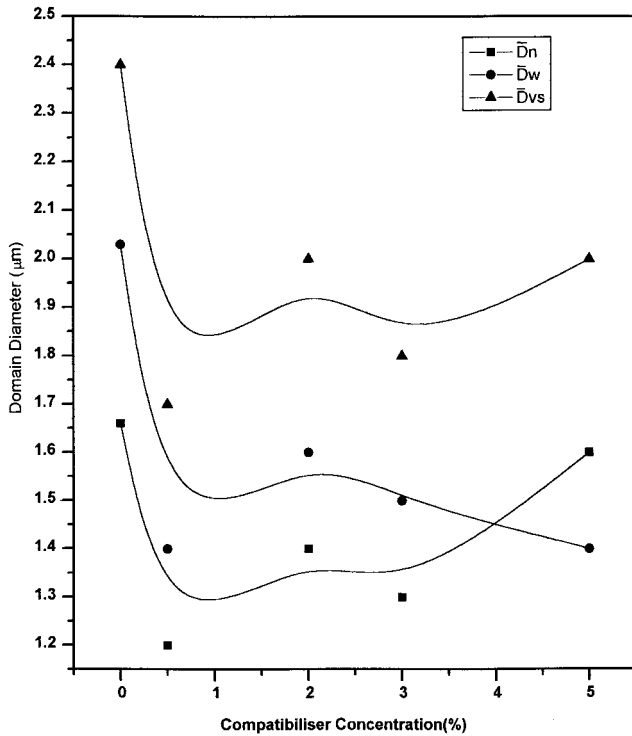
Figure 12 Effect of MA-*g*-LLDPE loading on dispersed domain diameter of E_{30} blend.

$$\frac{1}{\eta_{\text{blends}}} = \frac{\phi m'}{\eta m} + \frac{\phi d'}{\eta d} + \frac{\phi i'}{\eta i} - \left[\frac{1}{\eta m} - \frac{1}{\eta d}\right]\phi m'\phi d'$$

$$+ \left[\frac{\phi m'}{\eta m} - \frac{\phi d'}{\eta d}\right]\phi i' + \frac{\phi i'(\phi d' - \phi m'')}{\eta m} \quad (18)$$

where ϕ is the volume fraction, η is the viscosity, and the subscripts m, d, and i denote matrix, dispersed phase, and interface, respectively. It is clear from the above equation that the viscosity of the blends depends on the interface volume fraction and also on the viscosity of the interface. The leveling off in the viscosity-compatibilizer loading curve in MA-*g*-LLDPE and Ph-LLDPE may be understood from the morphology of the blends. SEM micrographs of the 70/30 blends compatibilized with Ph-LLDPE and MA-*g*-LLDPE are given in Figures 10 and 11. In both cases, as the concentration of the compatibilizer increases, the size of dispersed EVA phase decreases. About 0.5 to 1% compatibilizer concentration is found to be the optimum concentration in the case of MA-*g*-LLDPE. Beyond this concentration, MA-*g*-LLDPE causes a slight increase in size of dispersed domain and then levels off, maybe due to micelle formation in the continuous polyethylene matrix. The effect of compatibilizer (MA-*g*-LLDPE) loading on domain diameter is given in Figure 12. Scanning electron micrographs of the E_{70} blends at different shear rates are given in Figure 13. In these blends, EVA forms the continuous

phase and LLDPE forms the dispersed phase. From the SEM, it is clear that the particle size decreases with increasing shear rate. At high shear rate, the dispersed domains appear to be more uniformly distributed. The influence of shear rate on average domain diameter and polydispersity index of dispersed phase is depicted in Figure 14. It is observed that the average diameter of the dispersed domains decreases considerably with an increase in shear rate. The effect of shear rate on the morphology of compatibilized blends was also investigated. Figure 15 shows the effect of shear rate on the morphology of E30 blends compatibilized with 2% maleic anhydride compatibilizer. The diameter of more than 500 domains from the micrographs are measured and D_w, D_n, and D_{vs} are calculated. The values obtained are given in Table I. As the table reveals, there is no change in the diameter of the domains with shear rate, which indicates that compatibilization stabilizes morphology.

Effect of dynamic vulcanization

The physical properties of thermoplastic elastomers can be improved by vulcanization of the rubber phase during mixing.[45–47] This process, which is known as dynamic vulcanization, leads to a stable morphology, which has a uniform and fine distribution of the dispersed phase.

The effect of dynamic vulcanization on the viscosity of 70/30 EVA/LLDPE blends is given as a function of DCP content in Figure 16. Here, the viscosity of the crosslinked blend increases as a result of the addition of DCP up to 2%. After that, the viscosity almost levels off. Here also, the viscosity decreases with shear rate, showing pseudoplastic behavior. The morphology of the DCP vulcanized system is shown in Figure 17. In the DCP-cured system, the distribution of domain is finer and more uniform. The dispersed domain diameter and interfacial area per unit volume of different crosslinked samples are given in Table II. The size of the dispersed domain decreases considerably because of vulcanization and interfacial area increases. The degree of crosslinking was determined from swelling experiments by using the following relation:

$$\nu = \tfrac{1}{2}M_c \quad (19)$$

where ν is the degree of crosslinking and M_c is the molar mass between crosslinks. M_c was calculated by using the following Floryi–Rehner relation:

$$M_c = \frac{-\rho_p V_s V_0^{1/3}}{[\ln(1 - V_0) + V_0 + \chi V_0^2]} \quad (20)$$
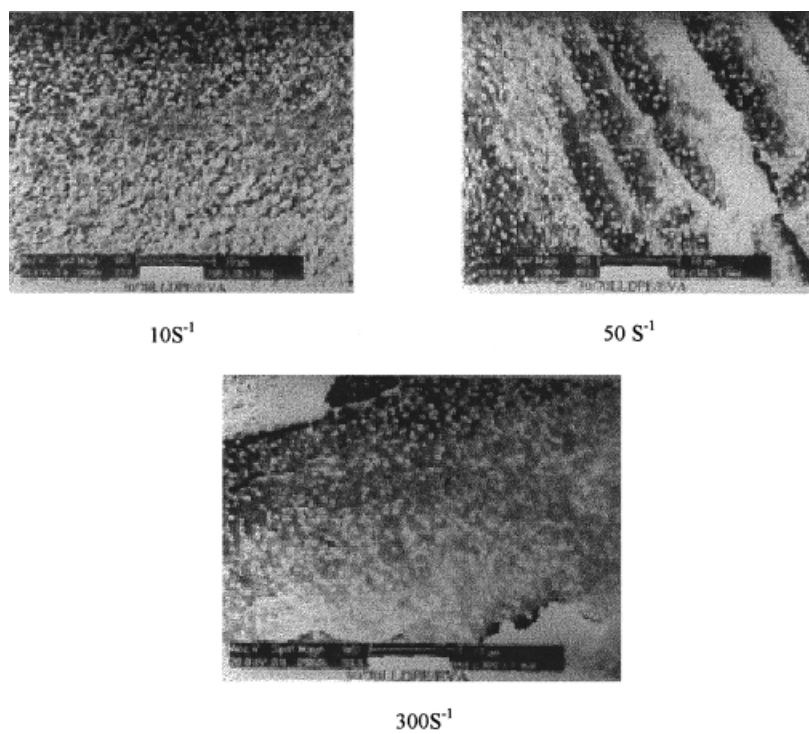
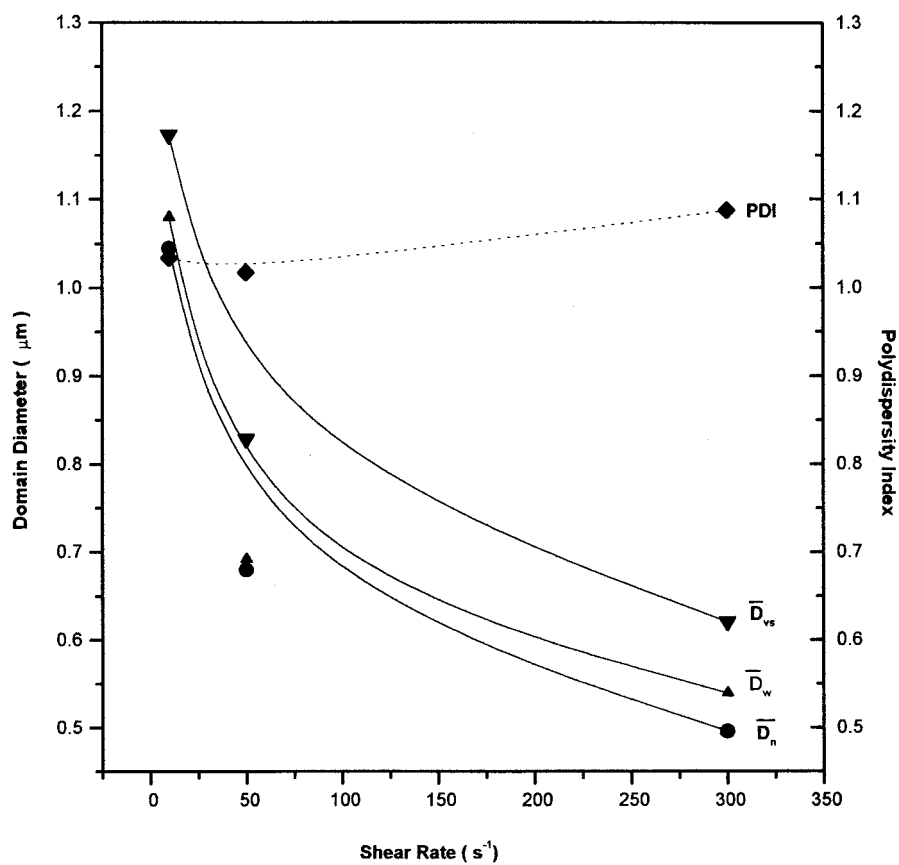Figure 13 SEM of E_{70} blends at different shear rates and at 150°C.

Figure 14 Effect of shear rate on dispersed domain diameter and polydispersity index of E_{70} blend.
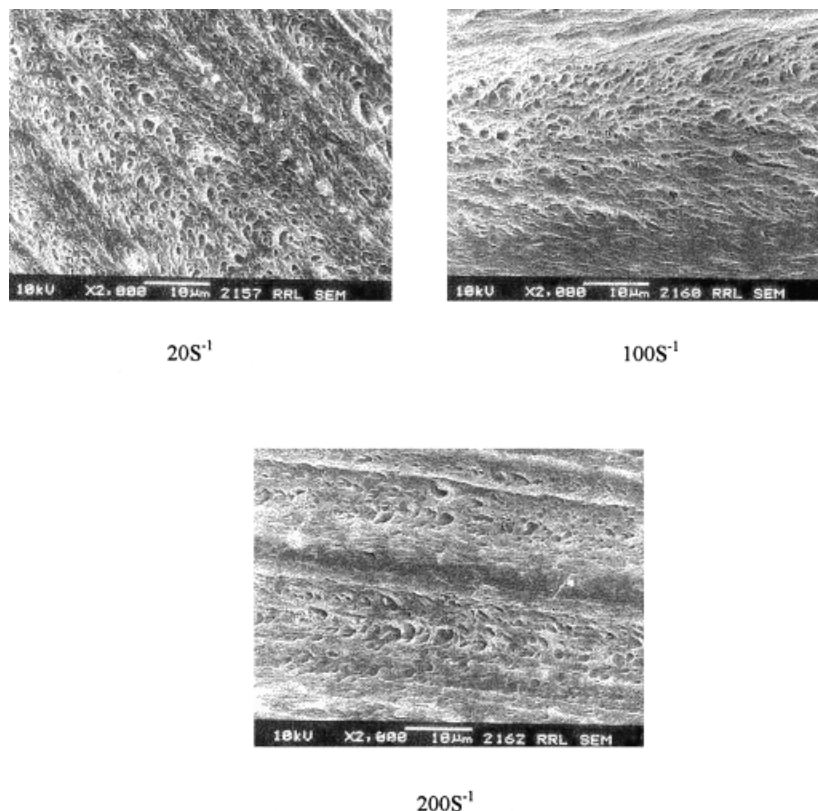
Figure 15 SEM of 2MC extruded at different shear rates and at 150°C.

where ρ_p is the density of the polymer; V_0 is the volume fraction of swollen rubber; χ is the interaction parameter; and V_s is the molar volume of the solvent. The values of ν obtained for 7EC1 and 7EC2 and 7EC3 are 1.119×10^{-4}, 1.553×10^{-4}, and 1.582×10^{-4}, respectively.

Effect of temperature

The dependence of the melt viscosity of LLDPE, EVA, and E_{30} blend on temperature is studied. The viscosities of both LLDPE and EVA decrease with an increase in temperature. The viscosity of the E_{30} blend also decreases with an increase in temperature. The activation energy was calculated from the plot of log η versus $1/T$ for E_0, E_{30}, and E_{100} blends. The activation energies are 1.35, 1.45, and 1.56 (KJ mol^{-1}) for E_0, E_{30}, and E_{100}, respectively. The activation energy of the blend increases with EVA concentration. Activation energy values are useful for fixing the processing methods and temperature.

TABLE I
Effect of Shear Rate on Dispersed Domain Diameter of 2MC Extruded at 150°C

Shear rate	$\bar{D}_n$ (μm)	$\bar{D}_w$ (μm)	$\overline{D_{vs}}$ (μm)
20	1	1.2	1.4
100	1	1.2	1.4
200	1	1.2	1.4
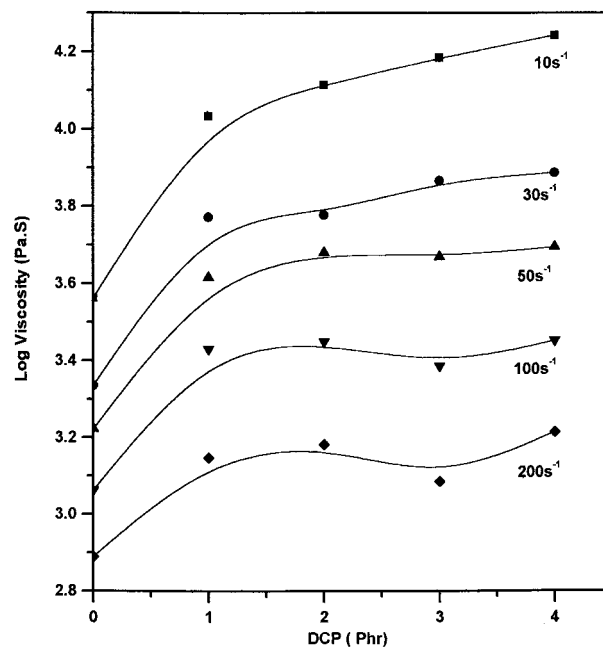
Figure 16 Effect of DCP loading on viscosity of E_{70} blend at different shear rates.
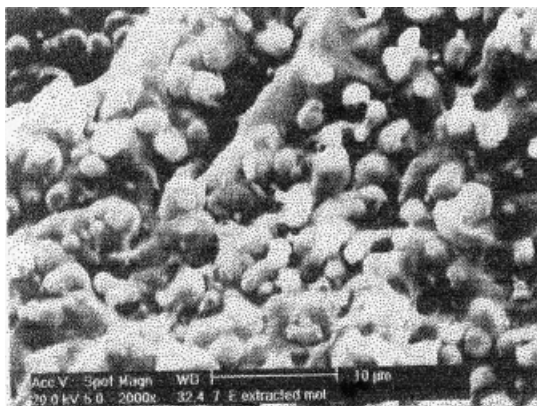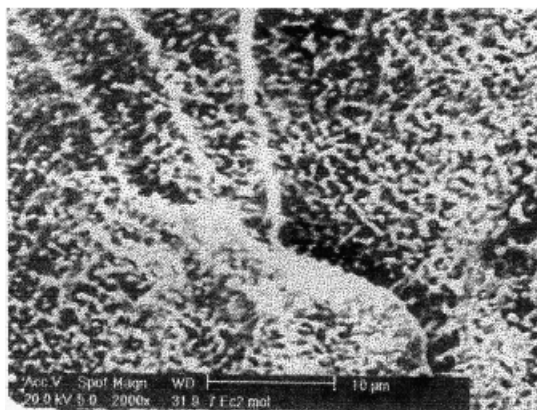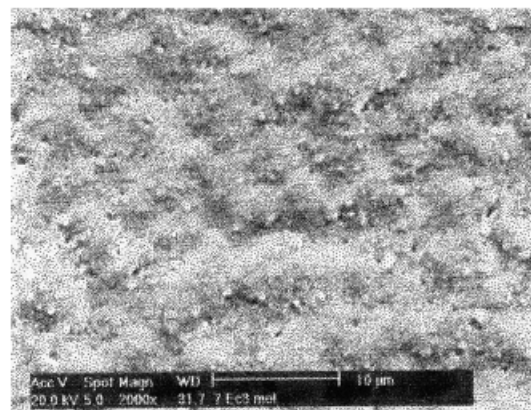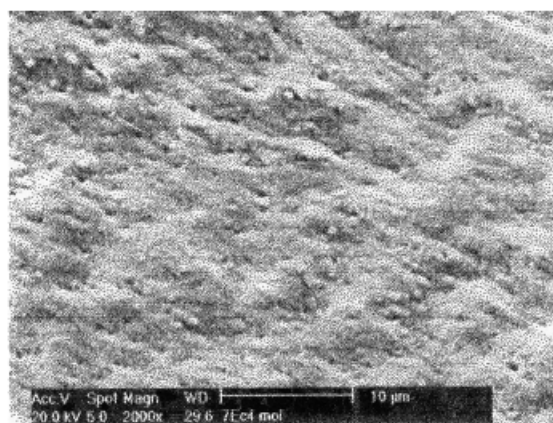
7E
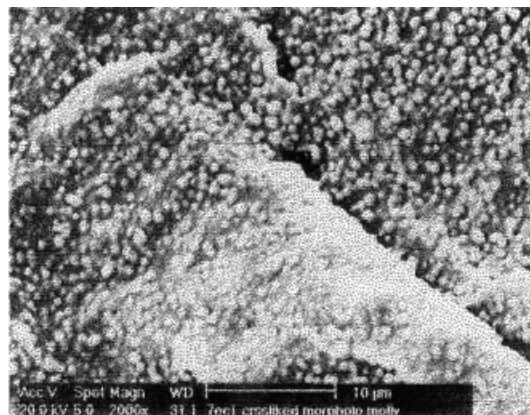
7EC$_1$

7EC$_2$

7EC$_3$

7EC$_4$

Figure 17 Effect of dynamic crosslinking on morphology of E_{70} blend.

TABLE II
Dispersed Domain Diameter and Interfacial Area/Unit Volume of E_{70} Blend and the Crosslinked Samples

Sample	$\bar{D}_n$ (μm)	Interfacial area/unit volume (μm^{-1})
7E	2.443	0.3731
$7EC_1$	0.7038	1.2950
$7EC_2$	0.5735	1.5891
$7EC_3$	0.5397	1.6887
$7EC_4$	0.4545	2.0053

Flow behavior index (n')

A simple understanding of the rheological behavior of polymeric materials is provided by the flow behavior index. Polymers with flow behavior index "n'" < 1 behave as a pseudoplastic material. The value for n' is 1 for Newtonian liquids. The effects of blend ratio, dynamic vulcanization, and compatibilization on flow behavior index of the samples were studied and the results are given in Table III. It is observed that the n' value decreases as the proportion of EVA in the blend increases. Further, the values are below 1, indicating the pseudoplastic nature of the EVA/LLDPE blends. The flow behavior index decreases considerably upon dynamic vulcanization, indicating increased pseudoplastic behavior, whereas compatibilization does not affect much on the flow behavior index.

Region of phase inversion

As observed from Figure 3, the change in viscosity ratio has a pronounced effect on the location of the region of phase inversion. Blending a high viscous material with a low viscous material causes the region of cocontinuity to shift toward a lower content of the low viscous phase. Favis and Chalifoux,[48] Elemans,[49] and Groeninckx et al.[50] report such observations.

We have tried to correlate experimental results with various theoretical equations, which point to the region of cocontinuity and phase inversion. Jordhamo et al.[51] developed an empirical model based on the melt viscosity ratio η_d/η_m and the volume fractions ϕ of each phase with a view to predict phase inversion

region in immiscible polymer blends. According to them, phase inversion should occur when the following equation holds

$$\eta_1 \phi_2 / \eta_2 \phi_1 = 1 \qquad (21)$$

Jordhamo's model, however, is limited to low shear rates and does not consider the effect of variations in the interfacial tension between the phases and eq. (21) does not always correctly predict the phase inversions, especially when blending materials with a large difference in melt viscosities. Chen and Su[52] have reported similar observations and they ascribed this discrepancy to the fact that eq. (21) overestimates the volume fraction of the high viscosity phase and proposed an alternative equation as follows:

$$\phi_{hv} / \phi_{1v} = 1.2(\eta_{hv} / \eta_{1v})^{0.3} \qquad (22)$$

where the subscript "hv" and "lv" denote the high and low viscosity phase, respectively. Chen and Su[52] explained the asymmetric equation as the result of post-mix coarsening, which depends mostly on the matrix viscosity; this effect will be more pronounced at compositions rich in the low viscous phase.

An even better description of the region of phase inversion is given when removing the factor 1.2 from eq. (22), as shown in eq. (23), which is Chen and Su's modified equation:

$$\phi_{hv} / \phi_{1v} = (\eta_{hv} / \eta_{1v})^{0.3} \qquad (23)$$

The theoretical composition of phase-inversion region calculated from eqs. (21), (22), and (23) by using viscosities obtained at shear rates 5–300 s^{-1} are given in Table IV. All the models give results agreeable with the experimental value. A comparison of the experimental results of LLDPE/EVA blends with eq. (22), the Chen and Su model shows the best correlation. The region of cocontinuity for LLDPE/EVA blends is between 40 and 60 volume fraction of EVA, which is supported by scanning electron micrographs.

TABLE III
Flow Behavior Index of Simple, Vulcanized, and Compatibilized Blends

Simple blends		Vulcanized samples		Compatibilized with MA-g-LLDPE		Compatibilized with Ph-LLDPE	
Samples	n'	Samples	n'	Samples	n'	Samples	n'
E_0	0.5373	7E	0.4829	3E	0.5207	3E	0.5207
E_{30}	0.5207	$7EC_1$	0.32304	0.5MC	0.5044	0.5PC	0.5074
E_{50}	0.5075	$7EC_2$	0.26008	2MC	0.5250	2PC	0.5026
E_{70}	0.4829	$7EC_3$	0.16244	5MC	0.4981	5PC	0.5044
E_{100}	0.4311	$7EC_4$	0.18314	10MC	0.5067	10PC	0.5093

TABLE IV
Results of Cocontinuity Modeling Studies

Shear rate (s^{-1})	LLDPE (Viscosity)	EVA (Viscosity)	LLDPE/ EVA (1)	EVA/LLDPE (2)	Jordhamo model (1)	Jordhamo model (2)	Chen and Su model	Chen and Su (modified)
5	6762.53	3717.50	1.819	0.5497	0.6451	0.3547	0.5894	0.5448
					0.3549	0.6453	0.4105	0.4552
10	5414.68	3420.86	1.58	0.6318	0.6124	0.3872	0.5792	0.5343
					0.3876	0.6128	0.4208	0.4657
20	4411.94	2290.75	1.926	0.5192	0.6593	0.3418	0.5936	0.5490
					0.3401	0.6582	0.4063	0.4510
30	3802.61	1880.56	2.022	0.4945	0.6691	0.3309	0.5971	0.5526
					0.3309	0.6691	0.4029	0.4474
50	3028.46	1396.00	2.169	0.4700	0.729	0.3155	0.6021	0.5578
					0.27100	0.6845	0.3978	0.4422
100	2123.97	936.78	2.267	0.4411	0.6939	0.3051	0.6054	0.5611
					0.3061	0.6939	0.3946	0.4389
200	1386.93	615.34	2.254	0.4437	0.6927	0.3073	0.6050	0.5607
					0.3073	0.6927	0.3950	0.4393
300	982.66	479.62	2.049	0.4880	0.6720	0.3243	0.5981	0.5536
					0.3279	0.6757	0.4019	0.4464

Region of cocontinuity from experimental results: 40–60-volume fraction of EVA.

CONCLUSION

The rheological properties of LLDPE/EVA blend systems were studied with special reference to the effect of blend composition shear rate, compatibilization, and dynamic vulcanization. The viscosities of all the blends decrease with increasing shear rate (i.e., the system exhibits a pseudoplastic behavior). At a given shear rate, the viscosity of the blends shows negative deviation due to interlayer slip between the phases. The flow behavior index, n', decreases with an increase in EVA content in the blend. The n' values of the blends are below 1, which is characteristic of pseudoplastic materials. The viscosities of these blends were correlated with various theoretical models and the Sood model lies closer to the experimental values. The compatibilization of these blends with phenolic-modified and maleic-modified LLDPE is found to increase the viscosity of the system, indicating an increase in interfacial interaction. The variation in viscosity was correlated with the morphology. Compatibilizer reduces the dispersed domain size and shows a leveling off at high concentrations. Dynamic vulcanization leads to uniform and even distribution of dispersed domains. Dynamic vulcanization increases the viscosity of the blends up to 2 Phr concentration of DCP, beyond which the viscosity levels off.

References

1. Caley, J. F.; Corossan, S. C. Polym Eng Sci 1988, 21, 249.
2. Mukhopadhyay, P.; Das, C. K. Plast Rubber Proc Appl 1988, 9, 141.
3. Heitmiller, R. F.; Naar, R. Z.; Zubusky, H. H. J Appl Polym Sci 1964, 8, 873.
4. Weeks, D. J.; Allen, W. J. Mech Eng Sci 1962, 4, 380.
5. Brydson, J. A. Flow Properties of Polymer Melts; George Godwin Ltd.: London, 1981.
6. Danesi, S.; Porter, R. S. Polymer 1978, 19, 448.
7. Utracki, L. A.; Kamal, M. R. Polym Eng Sci 1982, 26, 96.
8. Kim, Y. J.; Shin, G. S.; Lee, I. T.; Kim, B. K. J Appl Polym Sci 1993, 47, 295.
9. Koshy, A. T.; Kuriakose, B.; Premalatha, C. K.; Thomas, S. J Appl Polym Sci 1993, 49, 901.
10. Varkey, J. T.; Thomas, S.; Someswara, R. J Appl Polym Sci 1995, 56, 451.
11. George, J.; Ramamurthy, K.; Varughese, K. T.; Thomas, S. J Polym Sci, Polym Phys Ed 2000, 38, 1104.
12. George, S.; Ramamurthy, K.; Anand, J.S.; Groeninckx, G.; Varughese, K. T.; Thomas, S. Polymer 1999, 40, 4325.
13. Varghese, K. T.; De, P. P.; Nando, G. B.; De, S. K. J Vinyl Technol 1987, 9, 161.
14. Varghese, K. T. J Appl Polym Sci 1990, 39, 205.
15. Akhtar, S.; Kuriakose, B.; De, P. P.; De, S. K. Plast Rubber Process Appl 1987, 7, 119.
16. Kuriakose, B.; Kaust Gummi Kunsts 1984, 37, 1044.
17. Duvdevani, L.; Agaarwal, P. K.; Lundberg, R. D. Polym Eng Sci 1982, 22 (8), 499.
18. Kim, B. K.; Jeong, H. M.; Lee, Y. H. J Appl Polym Sci 1990, 40, 1805.
19. Miettinen, R. M. H.; Seppala, J. V.; Ikkala, O. T.; Reima, I. T. Polym Eng Sci 1994, 334 (5), 395.
20. Germain, Y.; Ernst, B.; Genelot, O.; Dhamini, L. J Rheol 1994, 38 (3), 681.
21. Valenza, A.; Acierno, D. Eur Polym J 1994, 30 (10), 1121.
22. Joshi, M.; Maiti, S. N.; Misra, A. J Appl Polym Sci 1992, 15, 1837.
23. Oommen, Z.; Premalatha, C. K.; Kuriakose, B.; Thomas, S. Polymer 1997, 38, 5611.
24. Okoroafar, E. U.; Villemuire, J. P.; Agassant, J. F. Polymer 1992, 33 (24), 5264.
25. Ha, C. S.; Kim, S. C. J Appl Polym Sci 1988, 35, 2211.
26. Kuriakose, B.; De, S. K. Polym Eng Sci 1988, 25 (10), 630.
27. Thomas, S.; Kuriakose, B.; Guptha, B. R.; De, S. K. Plast Rubber Proc Appl 1986, 6 (1), 85.
28. Han, P. K.; White, J. L.; Rubber Chem Technol 1995, 68, 728.

29. Coran, A.Y. In Handbook of Elastomers—Development and Technology; Bhowmick, A. K., Stephens, H. L., Eds.; Marcel Dekker: New York, 1988.
30. Varkey, J. T.; Rao, S. S.; Thomas, S. Polym Plast Technol Eng 1996, 35, 1.
31. Han, C. D.; Kim, Y. W. J Appl Polym Sci 1975, 19, 2831.
32. Shah, C. K. Polym Eng Sci 1976, 16, 742.
33. Carley, J. F. Reprints STP Reg Conf Plast Progr Proc 1980, 285.
34. Utracki, L. A.; Sammut, P. Polym Eng Sci 1988, 28, 1405.
35. Akhtar, S.; Kuriakose, B.; De, P. P.; De, S. K. Plast Rubber Proc Appl 1987, 7, 11.
36. Sood, R.; Kulkarni, M. G.; Dutta, A.; Meshelkar, R. A. Polym Eng Sci 1988, 28 (1), 20.
37. Oommen, Z.; Thomas, S; Nair, M. R. G. Polym Eng Sci 1996, 36, 151.
38. Asalatha, R.; Kumaran, G.; Thomas, S. Rubber Chem Technol 1995, 68, 671.
39. Brown, H. R.; Yang, A. C. M.; Russel, T. P.; Volksen, W.; Kramer, E. J. Polymer 1988, 29, 1807.
40. Yukioka, S.; Nagato, K.; Inoue, T. Polymer 1992, 33, 1171.
41. Felix, J. M.; Gatenholm, P. ACS Polym Mater Sci Eng Div Proc 67, Washington, DC, Aug. 1992.
42. Gatenholm, P.; Felix, J. M. New Advances in Polyolefins; Chung T. C., Ed.; Plenum Press: New York, 1993; p 237.
43. Sundarraj, U.; Macosko, C. W. Macromolecules 1995, 28 (8), 2647.
44. Chandramouli, K.; Jabarin, S. A. Adv Polym Technol 1995, 4 (1), 35.
45. Liao, F. S.; Su, A. C.; Hsu, T. C. J. Polymer 1994, 35, 2579.
46. Kuriakose, B.; De, S. K.; Bhagawan, S. S.; Sivaramakrishnan, R.; Athithan, S. K. J Appl Polym Sci 1986, 32, 5506.
47. Varughese, K. T.; De, P. P.; Sanyal, S. K. Die Angew Makromol Chem 1990, 182, 73.
48. Favis, B. D.; Chalifoux, J. P. Polymer 1988, 29, 1761.
49. Elemans, P. H. M. Ph.D. Thesis, TU Eindhoven, The Netherlands, 1989.
50. Everaert, V.; Aerts, L.; Groeninckx, G. Polymer 1999, 40, 6627.
51. Jordhamo, G. M.; Manson, J. A.; Sperling, L. H. Polym Eng Sci 1986, 26, 517.
52. Chen, T. H.; Su, A. C. Polymer 1993, 34, 4826.